Power System Reliability Evaluation Based on Sequential Monte Carlo Simulation Considering Multiple Failure Modes of Components

Wei Huang, *Student Member*, *IEEE*, Bo Hu, *Senior Member*, *IEEE*, Changzheng Shao, *Member*, *IEEE*, and Wei Li, Xiaozhe Wang, *Senior Member*, *IEEE*, Kaigui Xie, *Senior Member*, *IEEE*, and C. Y. Chung, *Fellow*, *IEEE*

***Abstract*—The component aging has become a significant concern worldwide, and the frequent failures pose a serious threat to the reliability of modern power systems. In light of this issue, this paper presents a power system reliability evaluation method based on sequential Monte Carlo simulation (SMCS) to quantify system reliability considering multiple failure modes of components. First, a three-state component reliability model is established to explicitly describe the state transition process of the component subject to both aging failure and random failure modes. In this model, the impact of each failure mode is decoupled and characterized as the combination of two state duration variables, which are separately modeled using specific probability distributions. Subsequently, SMCS is used to integrate the three-state component reliability model for state transition sequence generation and system reliability evaluation. Therefore, various reliability metrics, including the probability of load curtailment (PLC), expected frequency of load curtailment (EFLC), and expected energy not supplied (EENS), can be estimated. To ensure the applicability of the proposed method, Hash table grouping and the maximum feasible load level judgment techniques are jointly adopted to enhance its computational performance. Case studies are conducted on different aging scenarios to illustrate and validate the effectiveness and practicality of the proposed method.**

***Index Terms*—Power system, reliability evaluation, aging failure, sequential Monte Carlo simulation.**

I. Introduction

THE power system is recognized as one of the greatest engineering achievements of the 20th century, given its critical role in supplying continuous electricity to modern society [1]. However, as the system components installed decades ago have entered their wear-out stage, these systems have become less reliable [2], [3]. In recent years, blackouts caused by component aging failures have occurred frequently, posing a serious threat to economic development and quality of life. In 2023, an aging-induced blackout accident occurred in Pakistan, plunging 220 million users into darkness [4]. Furthermore, component aging can also present a significant threat to the transmission and full utilization of renewable energy. Therefore, improving the reliability of aged power systems and reducing their outage risk has become an essential task for power utilities [5], [6].

Thus, there is a pressing need to develop the methods that can accurately evaluate system reliability considering component aging failures. These methods could enable system planners to make appropriate reliability-centered maintenance plans to mitigate the adverse impacts of component aging failures on system reliability [7]. Some pioneering studies have been conducted in this regard.

Reference [8] proposes the first available method based on the non-sequential Monte Carlo simulation (NSMCS) method. In this method, equivalent unavailability (EU) is introduced to quantify the component reliability, representing the average probability of the component being available due to both random and aging failure modes. Similarly, an efficient mathematical quantification model is presented in [9] to evaluate the unavailability of the components by representing the bathtub curve as a Markov process [10]. Subsequently, NSMCS method is adopted for system reliability evaluation, where the operation states of components are randomly sampled based on their EUs. Although this method has been widely used due to its simplicity, it cannot capture the chronological property inherent in the aging failure characteristics of the components and the associated state transition process [11], [12]. As a result, the evaluated results may significantly deviate from reality [13].

To overcome the above limitations, several recent studies

Manuscript received: November 29, 2023; revised: March 2, 2024; accepted: June 14, 2024. Date of CrossCheck: June 14, 2024. Date of online publication: August 26, 2024.

This work was supported by the National Natural Science Foundation of China (No. 52022016), the Fundamental Research Funds for the Central Universities (No. 2023CDJYXTD-004), and the Graduate Research and Innovation Foundation of Chongqing (No. CYB22014).

W. Huang, B. Hu (corresponding author), C. Shao, and K. Xie are with the State Key Laboratory of Power Transmission Equipment Technology, School of Electrical Engineering, Chongqing University, Chongqing, China (e-mail: 17866628985@163.com; hboy8361@163.com; cshao@cqu.edu.cn; kaiguixie@vip.163.com).

W. Li is with China Southern Power Grid, Guangzhou, China (e-mail: liwei3@csg.cn).

X. Wang is with the Department of Electrical and Computer Engineering, McGill University, Montreal, Canada (e-mail: xiaozhe.wang2@mcgill.ca).

C. Y. Chung is with the Department of Electrical and Electronic Engineering, Hong Kong Polytechnic University, Hong Kong, China (e-mail: c.y.chung@polyu.edu.hk).

DOI: 10.35833/MPCE.2023.000939

have developed system reliability evaluation methods based on sequential Monte Carlo simulation (SMCS) (hereafter called SMCS-based system reliability evaluation method) to consider the time-related characteristics of the component aging failure mode [14]. In these studies, SMCS is used to sequentially sample the component operation states and the associated state duration from the component reliability model, simulating the chronology of the component state transition process. In this regard, the non-homogeneous poisson process (NHPP)-based two-state component reliability model is most widely used for describing and simulating the component state transition process considering aging failures [15]. In this model, the component state transition process is described as an interleaved sequence combination of the normal running and aging failure states. It assumes that the failed component can be as good as it is immediately before failure after applying repair activities. However, there are two deficiencies in this two-state component reliability model. First, component aging failures are generally non-repairable and once such failures occur, the failed component should be replaced with a new component [11]. Thus, the aging process fully stops in the failed components. Second, the aged components also transition from the normal running state to the failure state due to repairable random failures [16]. Nevertheless, this failure mode and its associated impact are obscured by the aging failure mode and are therefore not included in the two-state component reliability model. Therefore, applying this model for component state transition sequence generation (CSTSG) and subsequent system reliability will inevitably lead to erroneous results.

Consequently, it is necessary to develop a component reliability model that can accurately describe the state transition process of components considering non-repairable aging failure mode, while preserving the effects of the repairable random failure mode. However, this issue has not been investigated systematically.

There is another practical issue when using SMCS to incorporate the component aging failure mode in system reliability evaluation. Specifically, a significant number of repetitive simulations are generally required to adequately capture the stochastic behavior of component aging failures and obtain reliable reliability evaluation results [17]. During each simulation process, a large number of system states are generated, each of which must undergo minimum load-shedding calculations via the optimal power flow (OPF). This requirement inevitably leads to a heavy computational burden, thereby limiting the practical applicability of SMCS. This challenge will become more pronounced when evaluating power systems with a large number of aged components (potentially having more aging failures and requiring more simulations). Traditionally, various methods have been proposed to accelerate the SMCS process while maintaining desirable accuracy, including cross entropy-importance sampling (CE-IS) [18] and neural network based methods [19]. However, the time-varying nature of the reliability parameters of aged components makes it infeasible to use the CE-IS method to construct the optimal probability density function for efficient state sampling. Similarly, due to this constraint, it becomes unrealistic to build extensive training samples for the neural network to attain satisfactory specificity and sensitivity. In general, acceleration methods that are suitable for SMCSs considering component aging failures have been seldom investigated.

To address the aforementioned problems and difficulties, a systematic method is proposed to incorporate component aging failures in system reliability evaluation. At the component level, a three-state component reliability model is designed to refine the differentiated impacts of aging failures and random failures on the component state transition process. In this model, the impact of each failure mode is decoupled and characterized as the combination of two different state duration variables, which are clearly defined and modeled using suitable probability distributions. In this way, the state transition processes of the aged components can be efficiently simulated. At the system level, a general system reliability evaluation method considering component aging failures is established. This method employs SMCS for CSTSG and considers other chronological factors such as system load curves and spare components. To improve the computational performance of the proposed method, a two-step acceleration method is further developed. This method integrates Hash table (HT) grouping and maximum feasible load level (MFLL) judgment techniques to efficiently filter out the successful system state sampled in the SMCS process, thereby reducing the number of OPF solutions. Notably, this proposed method is also suitable for the reliability analysis of power systems with renewable energy integration.

Following the previous works in this field, this paper makes the following contributions.

1) A three-state component reliability model is designed to depict and simulate the component state transition process subject to repairable random failures and non-repairable aging failures. The involved four state duration variables are clearly defined and modeled using various probability distributions. Additionally, the impact of updated component replacement is also considered.

2) A general SMCS-based system reliability evaluation method is proposed to integrate the proposed three-state component reliability model for system reliability evaluation. It can generate various kinds of reliability indices, including probability, frequency, and expectation measures, for comprehensively quantifying the impact of multiple failure modes of the component. This model can also accommodate the renewable energy integration.

3) A two-step acceleration method is developed to improve the reliability evaluation efficiency by reducing the number of system states that require OPF analysis, which can enhance the computational performance of the proposed method, thus ensuring practical applicability and scalability.

The rest of the paper is organized as follows. Section II outlines the three-state component reliability model considering aging failures. Section III introduces the SMCS-based system reliability evaluation method. Section IV presents the proposed two-step acceleration method. Section V presents the case studies. Section VI discusses the work, and conclu-

sions are given in Section VII.

II. Three-state Component Reliability Model Considering Aging Failures

A. Conventional NHPP-based Two-state Component Reliability Model

The conventional NHPP-based two-state component reliability model is illustrated in Fig. 1, where t_1 is the time when the component is put back into operation; t_2 is the occurrence time of random failures; t_3 is the re-running time of repaired component; t_4 is the occurrence time of aging failures; t_5 is the commission time of new component; and TTF_{ran} and TTR_{ran} are the uptime and repair time, respectively.

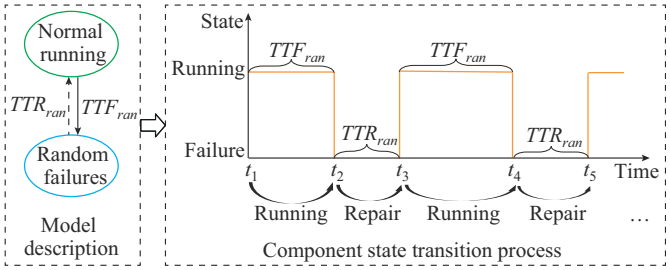

Fig. 1. Conventional NHPP-based two-state component reliability model.

The aging failures are assumed to be repairable; thus, the component state transition process is characterized by TTF_{ran} followed by TTR_{ran} [20]. Moreover, the duration of TTF_{ran} is assumed to follow the NHPP distribution, which tends to decrease over time considering the continuous increase in component aging degree [15]. However, this model cannot reflect the actual state transition process of the aged component due to the incorrect consideration of the aging failure characteristics and the neglect of the impact on random failures [11].

B. Design of a Three-state Component Reliability Model Based on Failure Mode Analysis

To construct a model that can describe the chronological state transition process of aged components subject to both random failure and aging failure modes, the characteristics of these two independent failure modes are analyzed and compared, as shown in Table I.

TABLE I
Characteristics of Aging Failure and Random Failure Modes

Factor	Aging failure mode	Random failure mode
Cause	It is mainly caused by the irreversible deterioration of component strength due to the long-term effects of multiple destructive stress	It is mainly caused by random operational mistakes or short-time incidents arising from unexpected operation and weather conditions
Feature	It exhibits a growth trend over running time	It is independent of component running time.
	It occurs only once during a component life cycle	It can repeatedly occur during a component life cycle
	The failed component must be replaced by a new one	The failed component can be restored by a sample repair

According to Table I, random failures are generally repairable and time-dependent, whereas aging failures are time-dependent, catastrophic, and non-repairable [16]. When aging failures occur, the failed component reaches the end of its life cycle and needs to be replaced by a new component [7]. Thus, the component aging process is fully stopped [21]. Before this, the aged component alternatively transitions between random failure and normal running states.

Thus, the actual component state transition process, which takes into account both aging and random failure modes, is shown in Fig. 2, where t_6 is the occurrence time of random failures; and t_7 is the re-running time of repaired component.

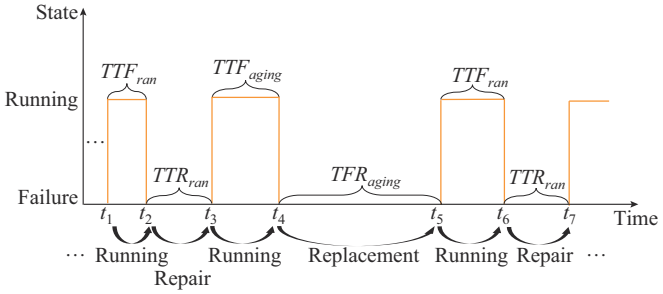

Fig. 2. Actual component state transition process.

According to Fig. 2, the component state transition process can be decomposed into two different working cycles that correspond to non-repairable aging and repairable random failure modes.

1) Cycle 1: a random failure occurs, transitioning the component from the running state to the random failure state. After being repaired, the component returns to its running state while continuing to age. This cycle includes two duration variables: TTF_{ran} and TTR_{ran}.

2) Cycle 2: aging failure occurs, forcing the component from the running state to the aging failure state. After being replaced, the component returns to the running state as a new component (the previous aging process stops). This cycle is characterized by two duration variables: TTF_{aging} (time to the aging failures) and TFR_{aging} (time to replacement).

Accordingly, a three-state component reliability model is designed to describe the state transition process of an aged component, as illustrated in Fig. 3.

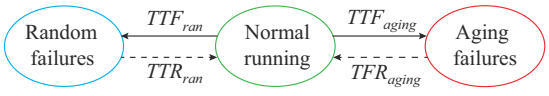

Fig. 3. Diagram of three-state component reliability model.

In this model, the random variables TTF_{ran}, TTR_{ran}, and TFR_{aging} typically adhere to time-independent probability distributions, as aging is not a concern for them (i.e., they are memoryless). In comparison, TTF_{aging} adheres to time-dependent probability distributions, considering the time-dependent characteristic of aging failures. Thus, different probability distributions are selected to model these four types of state duration variables in this paper, which are detailed in the following subsection.

C. Distribution Modeling of Four State Duration Variables

1) Modeling of TTF_{ran}

Random failures are aging-independent events caused by unexpected factors without memory, resulting in no relation to each failure event [16]. Thus, the exponential distribution is adopted here to model the TTF_{ran}, with its cumulative distribution function (CDF) given by:

$$F_{TTF_{ran}} = 1 - \exp(-\lambda_{ran} \cdot TTF_{ran}) \quad TTF_{ran} > 0 \tag{1}$$

where λ_{ran} is the parameter representing the constant random failure rate observed over historical statistical years.

2) Modeling of TTR_{ran}

The repair time, independent of the running time, may exhibit certain variability due to the efficiency of on-site work by repair personnel [22]. Therefore, the lognormal distribution, which has been verified across various power component types, is adopted here to characterize TTR_{ran} [23]. Its CDF is expressed as:

$$F_{TTR_{ran}} = \Phi\left(\frac{\ln TTR_{ran} - \mu_{ran}}{\sigma_{ran}}\right) \quad TTR_{ran} > 0 \tag{2}$$

$$\mu_{ran} = \ln(E(TTR_{ran})) - \frac{1}{2}\ln\left(1 + \frac{V(TTR_{ran})}{E(TTR_{ran})^2}\right) \tag{3}$$

$$\sigma_{ran}^2 = \ln\left(\frac{V(TTR_{ran}) + E(TTR_{ran})^2}{E(TTR_{ran})^2}\right) \tag{4}$$

where $\Phi(\cdot)$ is the CDF of the standard normal distribution; μ_{ran} and σ_{ran} are the location and scale parameters of $F_{TTR_{ran}}$, respectively; and $E(TTR_{ran})$ and $V(TTR_{ran})$ are the historical mean and variance of the component repair time, respectively.

3) Modeling of TFR_{aging}

The complete component replacement process consists of two time-consuming independent stages: order creation and component production, followed by transportation and installation [24]. Nevertheless, in cases where spare components are available, the replacement time can be reduced to the duration of the second stage exclusively. For this issue, two lognormal distributions are employed to model the time duration of these two stages separately, with their respective CDFs as follows:

$$F_{TFR_{aging}^{s_1}} = \Phi\left(\frac{\ln(TFR_{aging}^{s_1}) - \mu_{aging}^{s_1}}{\sigma_{aging}^{s_1}}\right) \quad TFR_{aging}^{s_1} > 0 \tag{5}$$

$$F_{TFR_{aging}^{s_2}} = \Phi\left(\frac{\ln(TFR_{aging}^{s_2}) - \mu_{aging}^{s_2}}{\sigma_{aging}^{s_2}}\right) \quad TFR_{aging}^{s_2} > 0 \tag{6}$$

where superscripts s_1 and s_2 denote the component order creation and production stage and the transportation and installation stage, respectively; and $\mu_{aging}^{s_1}$, $\sigma_{aging}^{s_1}$, $\mu_{aging}^{s_2}$, and $\sigma_{aging}^{s_2}$ can be estimated according to the historical replacement records of the component.

4) Modeling of TTF_{aging}

Unlike TTF_{ran}, TTR_{ran}, or TFR_{aging}, TTF_{aging} is dependent on the running time (asset age) of the component, as it represents the remaining lifetime of a component under its current asset ages [25]. As a result, TTF_{aging} of a component will follow time-dependent remaining lifetime distributions at different asset ages, reflecting the evolving likelihood of aging failures as the component ages.

In this case, it is necessary to first model the component lifetime distribution. Considering that aging failures occur with an extremely low probability (which can be assumed to be zero in engineering practice) before components enter their wear-out stage, an advanced three-parameter Weibull model is adopted to model the component lifetime distribution [26]. This model is defined here as T_{life}, and its CDF is given as:

$$F_{T_{life}} = \begin{cases} 1 - \exp\left(-\left(\dfrac{T_{life} - \eta_{aging}}{\alpha_{aging}}\right)^{\beta_{aging}}\right) & T_{life} \geq \eta_{aging} \\ 0 & T_{life} < \eta_{aging} \end{cases} \tag{7}$$

where α_{aging}, β_{aging}, and η_{aging} are the Weibull scale, shape, and threshold parameters estimated from historical aging failure data of the component, respectively. It is worth noting that the parameter η_{aging} has a clear physical meaning, as it represents the start time point of the wear-out stage of the component [27].

Based on (7), the remaining lifetime distribution for a component that is known to have survived until its current asset age T_{ser}, $F_{TTF_{aging}|T_{ser}}$, can be derived as:

$$\begin{aligned} F_{TTF_{aging}|T_{ser}} &= P(T_{life} \leq T_{ser} + TTF_{aging} | T_{life} > T_{ser}) = \\ &\frac{P(T_{life} \leq T_{ser} + TTF_{aging}) - P(T_{life} \leq T_{ser})}{1 - P(T_{life} \leq T_{ser})} = \\ &\frac{F_{T_{life}}(T_{ser} + TTF_{aging}) - F_{T_{life}}(T_{ser})}{1 - F_{T_{life}}(T_{ser})} \quad TTF_{aging} > 0 \end{aligned} \tag{8}$$

where $P(\cdot)$ denotes the corresponding probability.

Substituting (7) into (8), the analytical expression of $F_{TTF_{aging}|T_{ser}}$ can be obtained as:

$$F_{TTF_{aging}|T_{ser}} = \begin{cases} 1 - \dfrac{\exp\left(-\left(\dfrac{T_{ser} + TTF_{aging} - \eta_{aging}}{\alpha_{aging}}\right)^{\beta_{aging}}\right)}{\exp\left(-\left(\dfrac{T_{ser} - \eta_{aging}}{\alpha_{aging}}\right)^{\beta_{aging}}\right)} & T_{ser} \geq \eta_{aging} \\ 1 - \exp\left(-\left(\dfrac{T_{ser} + TTF_{aging} - \eta_{aging}}{\alpha_{aging}}\right)^{\beta_{aging}}\right) & T_{ser} < \eta_{aging} \end{cases} \tag{9}$$

D. State Duration Sampling Based on Inverse Transformation

In the process of generating subsequent component state transition sequences, it is necessary to use random values sampled from the above distribution model. Hence, analytical expressions of the sampling values for the TTF_{ran}, TTR_{ran}, TTF_{aging}, and TFR_{aging} state durations are further derived via inverse transformation sampling [28] as follows.

1) Sampling Value of TTF_{ran}

$$TTF_{ran,sam} = -\frac{-\mathrm{In}(U)}{\lambda_{ran}} \tag{10}$$

where U is the random variable.

2) Sampling Value of TTR_{ran}

$$TTR_{ran,sam} = \exp(\mu_{ran} + \sigma_{ran}\Phi^{-1}(U)) \tag{11}$$

where $\Phi^{-1}(U)$ denotes a random variable following a standard normal distribution.

3) Sampling Value of TFR_{aging}

Considering the impact of the spare component, the sampled TFR_{aging} is formulated under two different cases, which are given as follows.

When no spare components are available:

$$TFR_{aging,sam} = \exp(\mu_{aging}^{s_1} + \sigma_{aging}^{s_1}\Phi^{-1}(U)) + \exp(\mu_{aging}^{s_2} + \sigma_{aging}^{s_2}\Phi^{-1}(U_1)) \tag{12}$$

Alternatively, if a spare component is available, we can obtain:

$$TFR_{aging,sam} = \exp(\mu_{aging}^{s_2} + \sigma_{aging}^{s_2}\Phi^{-1}(U_1)) \tag{13}$$

where the random variable U_1 is also uniformly distributed in the interval (0,1).

4) Sampling Value of TTF_{aging}

Let the current asset age of the component be T_{ser} ($T_{ser} \geq 0$); therefore, $TTF_{aging,sam}$ can be expressed as:

$$TTF_{aging,sam} = \alpha_{aging}(-\mathrm{In}((1-\Im)U))^{\frac{1}{\beta_{aging}}} + \eta_{aging} - T_{ser} \tag{14}$$

$$\Im = F_{T_{life}}(T_{ser}) = \begin{cases} 1 - \exp\left(-\left(\dfrac{T_{ser} - \eta_{aging}}{\alpha_{aging}}\right)^{\beta_{aging}}\right) & T_{ser} \geq \eta_{aging} \\ 0 & T_{ser} < \eta_{aging} \end{cases} \tag{15}$$

The aforementioned three-state component reliability model is applicable to various types of power components, including generating units, transformers, and transmission lines. However, each component type should have an individual set of model parameters, which requires the estimation from the respective historical data. Note that this model assumes that one component that is in aging failure mode needs to be completely replaced.

Furthermore, in practical engineering scenarios, infrastructure managers of aging power system might replace aging-failed components with updated ones, which could have different reliability parameters from the original components. Regarding this issue, a random based component type selection method can be employed to determine the specific component type for replacement (whether original or updated). Subsequently, the parameters used in three-state component reliability model will be updated accordingly for the subsequent state duration sampling.

III. General SMCS-based System Reliability Evaluation Method

The proposed method is based on the SMCS and includes four parts: component state sequence generation, system state sequence generation, system state analysis, and process of proposed SMCS-based system reliability evaluation method. These parts are introduced in detail as follows.

A. Component State Sequence Generation

Considering the competitive relationship between aging failure and random failure modes during the component operation process, it is crucial to determine the next cycle (failure mode) before conducting chronological state sequence sampling. Here, the failure event with the earliest arrival time is selected as the next failure. Specifically, if $TTF_{aging,sam}$ is smaller than $TTF_{ran,sam}$, the next failure event is identified as an aging failure and random failures will not occur before this failure [29]. The detailed procedure for generating the component state sequence using SMCS is outlined in Procedure I. Note that the impact of sharing component spares and updated component replacement is also considered in this procedure.

Procedure I: component state sequence generation

Input: component reliability parameters (D_{total} is the predefined simulation horizon).

Output: generated component state sequence.

Step 1: initialization. Assume that the component is in the normal running state at the initial time; let the simulation time $TL_{sim} = 0$.

Step 2: calculate/update the remaining lifetime distribution of a component at its current asset age according to (8).

Step 3: determine the time duration to the next state transition of the component, d_{sim}, according to the following step.

1) Sample the uptime if the next state is a failure state.
Determine the next failure mode and value d_{sim} using (10), (14), and (16). Then, go to *Step 4*.

$$d_{sim} = \begin{cases} TTF_{aging,sam} & TTF_{ran,sam} > TTF_{aging,sam} \\ TTF_{ran,sam} & TTF_{ran,sam} \leq TTF_{aging,sam} \end{cases} \tag{16}$$

2) Sample the downtime if the next state is a normal running state.
a) Check if the current failure is a random failure. If so, sample d_{sim} using (11); otherwise, go to b)-d).
b) Determine the component type that is used for replacement.
c) Update the component reliability parameters, including λ_{ran}, μ_{ran}, σ_{ran}, μ_{aging}^{s1}, σ_{aging}^{s1}, μ_{aging}^{s2}, σ_{aging}^{s2}, α_{aging}, β_{aging}, and η_{aging}.
d) Check if there is a spare component available at present. If there is, sample d_{sim} using (13); otherwise, use (12).

Step 4: accumulate the simulation time:

$$TL_{sim} = TL_{sim} + d_{sim} \tag{17}$$

Step 5: check whether TL_{sim} reaches D_{total}. If not, update T_{ser} and return to *Step 3* (note that T_{ser} will be redefined as 0 after the component is replaced); otherwise, go to *Step 6*.

Step 6: output the generated component state sequence.

B. System State Sequence Generation

During the operation of power systems, changes in either the component state sequence or system load level will trigger system state transitions. Consequently, the following two steps are employed to generate the chronological system state sequence.

Step 1: generate and combine the state sequences of all components on the same time basis using Procedure I.

Step 2: extract all the system states and partition those with multiple load levels into several contiguous states.

The process of generating the system state sequence for three components (C_1-C_3) and three load levels (L_s: L_1-L_3) based on the SMCS is illustrated, as shown in Fig. 4. Curve S_1 represents the obtained system state sequences after implementing *Step 1*. Curve S_2 represents the required system state sequences considering both changes in the component

state sequence and system load level. Indices 1-15 correspond to 15 individual system states.

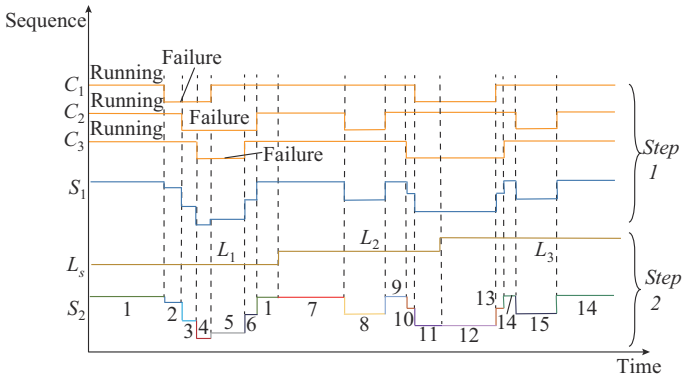

Fig. 4. Illustration of state sequence generation process based on SMCS.

C. System State Analysis

Following the system state sequence generation, this subsection focuses on the analysis and evaluation of the adequacy of each system state within the sequence. To this end, an OPF model is formulated to minimize load curtailment by readjusting generation outputs to maintain system/bus power balance, alleviate line/transformer overloads, and prevent load shedding if feasible. In this paper, bus loads are assumed to be fully correlated with the total system load [30]. Therefore, for a given system state s, let its corresponding component state vector and time duration be $\boldsymbol{v}_s$ and d_s, respectively. This model can be expressed as:

$$\min LC_s = \sum_{i \in \Psi_{bus}} P_{s,i} \tag{18}$$

s.t.

$$\sum_{g \in \Psi_{g,i}} P_{s,g} + \sum_{r \in \Psi_{i,in}} PL_{s,r} - \sum_{r \in \Psi_{i,out}} PL_{s,r} = L_{s,i} P_{i,peak} - P_{s,i} \quad i \in \Psi_{bus} \tag{19}$$

where Ψ_{bus}, $P_{s,i}$, and LC_s are the set of system buses, the load-shedding value on bus i, and the total system load-shedding value under system state s, respectively; $P_{i,peak}$ is the peak load demand on bus i; $P_{s,g}$ and $PL_{s,r}$ are the outputs of generator g and the power flow on branch r, respectively; $L_{s,i}$ is the load ratio of bus i; and $\Psi_{g,i}$, $\Psi_{i,in}$, and $\Psi_{i,out}$ are the sets of generators (traditional generators or wind/solar generators) connected to bus i, the sets of branches flowing into bus i, and the sets of branches flowing out of bus i, respectively.

$$\sum_{g \in \Psi_g} P_{s,g} + \sum_{i \in \Psi_{bus}} P_{s,i} = L_{s,i} \sum_{i \in \Psi_{bus}} P_{i,peak} \tag{20}$$

$$PL_{s,r} = b_r(\theta_{s,i} - \theta_{s,j}) \quad r \in \Psi_{branch} \tag{21}$$

where $\theta_{s,i}$ and $\theta_{s,j}$ are the voltage angles of bus i and bus j, respectively; b_r is the admittance of branch; and Ψ_{branch} is the set of branches.

$$0 \le P_{s,i} \le L_{s,i} P_{i,peak} \quad i \in \Psi_{bus} \tag{22}$$

$$-v_{s,r} \cdot \overline{PL_r} \le PL_{s,r} \le v_{s,r} \cdot \overline{PL_r} \quad r \in \Psi_{branch}, v_{s,r} \in \{0,1\} \tag{23}$$

$$0 \le PG_{s,g} \le v_{s,g} \cdot \overline{PG_g} \quad g \in \Psi_g, v_{s,g} \in \{0,1\} \tag{24}$$

where $v_{s,r}$ and $v_{s,g}$ are the indicator variables for a component (if one component is in the failure state, the indicator variable equals 0; otherwise, the indicator variable equals 1); and $\overline{PL_r}$ and $\overline{PG_g}$ are the maximum available capacities of branch r and generator g, respectively.

Constraint (19) is the power balance equation for each bus. Constraint (20) states the system power balance. The DC power flow model is expressed as (21) in terms of the bus angles and reactance. Constraint (22) represents the load-shedding limits on each bus. Constraint (23) states the power limits of branches. Constraint (24) is the available capacity range of the generators.

$LS_s > 0$ indicates that system state s has a load loss. Therefore, its label indicator J_s is set to be 1; otherwise, J_s is set to be 0. Throughout every SMCS process, the calculation results for each system state are recorded for the following reliability index calculations.

To comprehensively quantify the system reliability performance, three reliability indices suitable for composite generation and transmission systems are employed in this paper [31]. Assuming that the evaluation horizon is D_{total} and the total number of simulations is K_{sam}, these indices can be expressed as follows.

1) Probability of load curtailment (PLC): this index is used to measure the probability of system failure.

$$PLC = \frac{\sum_{k=1}^{K_{sam}} PLC_k}{K_{sam}} = \frac{\sum_{k=1}^{K_{sam}} \left(\frac{1}{D_{total}} \sum_{s \in \Theta_k} J_s d_{k,s} \right)}{K_{sam}} \tag{25}$$

where $d_{k,s}$ is the duration of system state s in the k^{th} simulation; and Θ_k is the set of system states obtained from the k^{th} simulation.

2) Expected frequency of load curtailment (EFLC): this index is used to measure the number of occurrences of transition from a success state to a failure state in the system state sequence.

$$EFLC = \frac{\sum_{k=1}^{K_{sam}} EFLC_k}{K_{sam}} = \frac{\sum_{k=1}^{K_{sam}} \left(\sum_{s \in \Theta_k} I_{k,s} \right)}{K_{sam}} \tag{26}$$

where $I_{k,s}$ is an indicator variable. If the system state s is a state with load loss and its predecessor is a state without load loss, $I_{k,s} = 1$; otherwise, $I_{k,s} = 0$.

3) Expected energy not supplied (EENS): this index is used to measure the expected amount of load shedding.

$$EENS = \frac{\sum_{k=1}^{K_{sam}} EENS_k}{K_{sam}} = \frac{\sum_{k=1}^{K_{sam}} \left(\sum_{s \in \Theta_k} J_s d_{k,s} \cdot LS_s \right)}{K_{sam}} \tag{27}$$

Note that the other indices such as the expected duration of load curtailment (EDLC) and average duration of load curtailment (ADLC) can be derived from (25)-(27) without any additional difficulty [32].

D. Process of Proposed SMCS-based System Reliability Evaluation Method

Procedure II summarizes the workflow of the proposed method. The stopping criterion is when the coefficient of

variance (COV) of *EENS* β_{EENS} is less than a preset value $\beta_{\max}$.

Procedure II: SMCS-based system reliability evaluation

Input: system data include topology information, load data, component reliability parameters D_{total} and $\beta_{\max}$.
Output: system reliability indices *PLC*, *EFLC*, *EENS*.

1) SMCS-based system state sequence generation
Step 1: input all the system data, assume that all the components are in running states initially, and let $k=1$.
Step 2: start the k^{th} simulation. The state sequences of all the components are simulated over the evaluation horizon on the same time basis (refer to Section III-A).
Step 3: construct the chronological system state sequence by combining the state sequences of all components and the chronological load (refer to Section III-B).
2) System state analysis
Step 4: extract all system states within the generated system state sequence and save them in set Θ_k.
Step 5: calculate the load curtailment of each system state based on (18)-(24) (refer to Section III-C).
3) Calculation and updating of reliability index
Step 6: update the system reliability indices after k simulations according to (25)-(27) (refer to Section III-D).
Step 7: calculate β_{EENS} and judge whether the evaluation results are acceptable [17].

$$\beta_{EENS}=\frac{1}{EENS}\sqrt{\frac{1}{k(k-1)}\sum_{h=1}^{k}(EENS_h-EENS)^2} \tag{28}$$

If $\beta_{EENS}>\beta_{\max}$, let $k=k+1$ and restore all the input data; repeat *Step 2* to *Step 5*. Otherwise, terminate the evaluation process and output the final system reliability indices.

As shown in the Procedure II, this method necessitates repeated OPF calculations for each system state sampled in every SMCS process. For an old power system with a large number of aged components, this requirement may lead to prohibitively high computational costs [3]. Consequently, the following section concentrates on developing efficient two-step acceleration method and integrating it into this procedure.

IV. Two-step Acceleration Method for System Reliability Evaluation

During the iterative SMCS process, most sampled system states belong to the success category (no load curtailments); therefore, they do not contribute to the computation of system reliability indices. Therefore, this section introduces a two-step acceleration method to quickly identify successful system states in every SMCS process, consequently reducing the number of system states requiring OPF computations. The basic structure of this two-step acceleration method is shown in Fig. 5, which includes the following two steps.

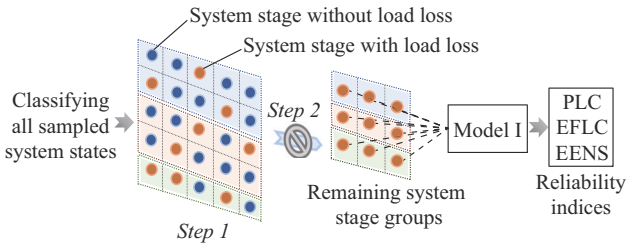

Fig. 5. Basic structure of proposed two-step acceleration method.

Step 1: system state grouping. This step focuses on classifying the sampled system states with identical component state vectors into corresponding groups using an HT technique.

Step 2: system state filtering. This step focuses on rapidly filtering out system states within each group that do not result in load loss by employing the MFLL.

By implementing these two steps, only the remaining system states require OPF solutions, which greatly reduces the required evaluation time.

As explained in Section III, a system state includes two features: the component state vector and the system load level vector. Due to the characteristics of chronological simulation, numerous system states sampled in each SMCS process share identical component state vectors but differ only in their system load levels [17]. Each component state vector is associated with a unique MFLL value, which represents the highest load level that the system can sustain without triggering load shedding. Inspired by this, this subsection utilizes the MFLL values to judge whether system states with the same component state vector would result in load loss without requiring individual OPF analyses. Specifically, system states with load levels lower than their corresponding MFLL values can be directly identified as successful system states.

To achieve this, an HT-based system state grouping is used to categorize the sampled system states with the same component state vectors into the same groups. The involved steps are summarized, as shown in Procedure III.

Procedure III: HT-based system state grouping

Input: sampled system states in the k^{th} SMCS process.
Output: the system state grouping results.

Step 1: initialization. An empty HT χ_{ht} is created to store the system state grouping results.
Step 2: generate the hash key of each system state based on its component state vector $\boldsymbol{v}$ using the Hash key function.
Step 3: insert each system state into χ_{ht}. Place the system states with the same Hash key in the same linked list in χ_{ht}.
Step 4: output the system state groups in the order of the generated Hash keys.

After grouping the sampled system states, the next step is to determine the value of the MFLL, i.e., LT_{syst}, related to each system state group. For this purpose, an optimization model formulated in [33] is adopted. Let $LT_{syst|\boldsymbol{v}_{sg}}$ denote the MFLL value corresponding to group *sg* with component state vector $\boldsymbol{v}_{sg}$. The optimization model is expressed, as shown in Model I.

Model I: determination of MFLL

$$\max LT_{syst|\boldsymbol{v}_{sg}} \tag{29}$$

s.t.

$$\sum_{g\in\Psi_{g,i}}P_{g|\boldsymbol{v}_{sg}}+\sum_{r\in\Psi_{t,in}}PL_{r|\boldsymbol{v}_{sg}}-\sum_{r\in\Psi_{t,out}}PL_{r|\boldsymbol{v}_{sg}}=LT_{syst|\boldsymbol{v}_{sg}}\cdot P_{i,peak}\quad i\in\Psi_{bus} \tag{30}$$

$$\sum_{g\in\Psi_g}P_{g|\boldsymbol{v}_{sg}}=LT_{syst|\boldsymbol{v}_{sg}}\sum_{i\in\Psi_{bus}}P_{i,peak} \tag{31}$$

$$b_r(\theta_{i|\boldsymbol{v}_{sg}}-\theta_{j|\boldsymbol{v}_{sg}})\le\left|\upsilon_{r|\boldsymbol{v}_{sg}}\right|\cdot\overline{PL_r}\quad r\in\Psi_{branch},\upsilon_{r|\boldsymbol{v}_{sg}}\in\{0,1\} \tag{32}$$

$$0\le PG_{g|\boldsymbol{v}_{sg}}\le\upsilon_{g|\boldsymbol{v}_{sg}}\cdot\overline{PG_g}\quad g\in\Psi_g,\upsilon_{g|\boldsymbol{v}_{sg}}\in\{0,1\} \tag{33}$$

$$-\upsilon_{r|\boldsymbol{v}_{sg}}\cdot\overline{PL_r}\le PL_{r|\boldsymbol{v}_{sg}}\le\upsilon_{r|\boldsymbol{v}_{sg}}\cdot\overline{PL_r}\quad r\in\Psi_{branch},\upsilon_{r|\boldsymbol{v}_{sg}}\in\{0,1\} \tag{34}$$

Equations (29) - (34) represent the power balance, power generator output, and line flow constraints, respectively. Once the value of $LT_{syst|v_{sg}}$ is obtained, the successful system states within the system state group *sg* can be filtered out.

Finally, Fig. 6 gives the overall flowchart of the proposed SMCS-based system reliability evaluation method with the two-step acceleration method.

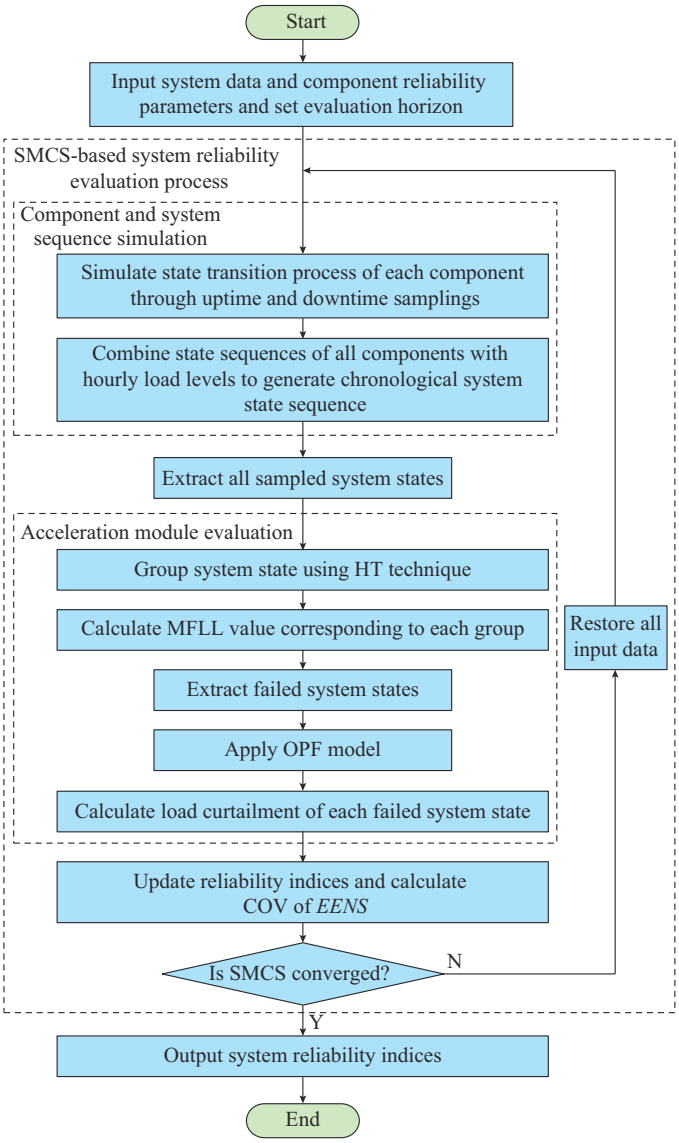

Fig. 6. Overall flowchart of proposed SMCS-based system reliability evaluation method with two-step acceleration method.

V. Case Studies

In this paper, various case studies are performed to validate the accuracy and efficiency of the proposed SMCS-based system reliability evaluation method.

A. Basic Test System Description and Simulation Setting

The modified RTS-79 system (MRTS-79) includes 24 buses, 32 generating units, 33 transmission lines, and 5 transformers, with a total generating capacity of 3405 MW and a peak load of 2850 MW. This system is geographically divided into three regions, R1, R2, and R3, as shown in Fig. 7.

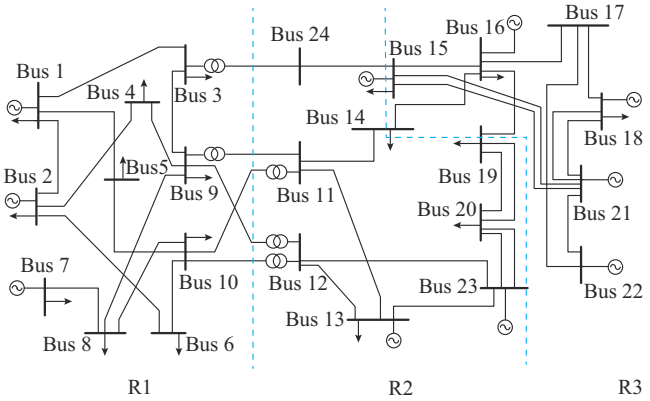

Fig. 7. Network topology of MRTS-79.

For all cases, the evaluation horizon is set to be one year. $\beta_{\max}$ for SMCS is set to be 0.05, which has been demonstrated to ensure reasonable accuracy [34]. The parameters for the state duration distributions of each power component type are summarized in Supplementary Material A. These parameters are mainly derived from the statistical data provided in [6], [35], [36] using the maximum likelihood estimation, which has been proven to have greater precision than other parameter estimation methods [26]. It is worth noting that the time required for power transformers, generating units, and ordering and production of transmission line is assumed to be 75% of their total replacement time [37], [38]. As discussed in Section III-A, different reliability parameters can also be used in the proposed method without adding difficulty in practical engineering.

B. Reliability Analysis of Basic Test System

This subsection focuses on evaluating the system reliability under various aging degrees using the proposed method. For simplicity, the annualized system reliability indices are calculated for analysis, i.e., the system load level remains at 2850 MW [32]. The most widely used NSMCS method presented in [8] is adopted for comparison. This method does not consider the chronological operation process of aged components when evaluating system reliability indices. Note that the spare component strategy is also ignored to ensure a fair comparison.

Considering the increase in the system aging degree over time, ten scenarios with different aging regions and component asset ages are specifically designed for comprehensive analysis, as detailed in Table II. It is assumed that components of the same type within the same region have identical asset ages. The asset ages of all components within nonaged regions are set to be 10 years. Note that scenario 1 is specifically designed to simulate a system without aging effects.

Table III provides the annualized PLC and EENS indices for the 10 scenarios obtained from the proposed method and the NSMCS method.

According to Table III, the following key observations can be made.

1) The system reliability indices exhibit a significant increase as both the number and asset ages of aged components increase. For example, the annualized PLC in aging

scenarios 6 and 9 increases by 51.613% and 109.67%, respectively, compared with the value obtained from basic scenario 1. Similarly, the annualized EENS indices in these two scenarios also increase by 63.375% and 137.023%, respectively. These observations are expected, as the occurrence of component aging failures tends to increase as the system aging degree increases. These findings provide quantitative evidence of the significant influence of component aging failures, indicating that they are the dominant factor contributing to the unreliability of aged power systems.

TABLE II
DESCRIPTION OF TEN SYSTEM SCENARIOS

Scenario No.	Aging region	Current asset age of aged component (year)		
		Generating unit	Power transformer	Transmission line
1		10	10	10
2	R1	48	42	45
3	R1	51	47	50
4	R1	54	52	55
5	R1, R2	48	42	45
6	R1, R2	51	47	50
7	R1, R2	54	52	55
8	R1, R2, R3	48	42	45
9	R1, R2, R3	51	47	50
10	R1, R2, R3	54	52	55

TABLE III
ANNUALIZED PLC AND EENS INDICES FOR TEN SCENARIOS

Scenario No.	PLC		EENS (MWh/year)	
	NSMCS	Proposed	NSMCS	Proposed
1	0.031	0.031	3.514×10^{4}	3.512×10^{4}
2	0.036	0.032	4.013×10^{4}	3.627×10^{4}
3	0.047	0.034	5.037×10^{4}	4.025×10^{4}
4	0.084	0.037	9.401×10^{4}	4.459×10^{4}
5	0.045	0.033	5.130×10^{4}	3.728×10^{4}
6	0.093	0.047	1.151×10^{5}	5.741×10^{4}
7	0.217	0.078	3.303×10^{5}	9.645×10^{4}
8	0.056	0.040	6.609×10^{4}	4.715×10^{4}
9	0.146	0.065	2.176×10^{5}	8.329×10^{4}
10	0.363	0.128	7.691×10^{5}	1.881×10^{5}

2) Across scenarios 2 to 10, the NSMCS generally yields larger PLC and EENS indices than the proposed method. Moreover, the discrepancy between these two methods tends to increase as the system aging degree becomes more pronounced. For example, in scenario 10, the PLC and EENS indices obtained from the NSMCS are 2.836 times and 4.089 times greater, respectively, than those of the proposed method. The main reason behind this is that the NSMCS disregards the sequential operation behaviors of the component and makes the erroneous assumption that aging-failed components will be completely unavailable during the remaining evaluation horizon. Accordingly, if power utilities still use NSMCS, there is a great risk of underestimating the actual system reliability level.

Since the NSMCS is unable to accurately estimate the annualized EFLC indices, only the EFLC results obtained from the proposed method are provided, as shown in Table IV.

TABLE IV
ANNUALIZED EFLC RESULTS OF MRTS-79 IN DIFFERENT AGING SCENARIOS

Scenario No.	EFLC (occurrence/year)	Scenario No.	EFLC (occurrence/year)
1	6.145	6	7.592
2	6.158	7	9.683
3	6.270	8	7.063
4	6.535	9	8.776
5	6.160	10	10.958

One notable observation from Table III and Table IV is the greater growth rate in the PLC and EENS indices compared with the EFLC index as the system aging degree increases. For instance, the PLC and EENS indices of scenario 7 increase by 151.613% and 174.474%, respectively, while the EFLC index increases by only 42.514% compared with the value in basic scenario 1. Similar trends can be observed in other aging scenarios. These findings are reasonable since component aging failures will lead to a longer system outage duration and greater load losses than random failures. Consequently, it can be inferred that using the two-state component reliability model established in [15] for system reliability evaluation is inadequate. This is because the two-state component model fails to describe and distinguish the differentiated impacts of component aging and random failure modes.

In summary, the above observations reveal the significant impact of component aging failures on system reliability. It is also evident that incorporating the proposed three-state component reliability model in the system reliability evaluation is crucial for realizing a more reliable and accurate evaluation of the system reliability level.

C. Efficiency Analysis of Proposed Method with Two-step Acceleration Method

The computational performance of the proposed method with the two-step acceleration method is crucial for its practical implementation in real systems. This subsection focuses on the verification of the computational efficiency of the proposed method with the two-step acceleration method by conducting an annual reliability analysis on scenarios 9 and 10. The RTS 8736-hour load data are used as the annual system load curve. The crude sequential Monte Carlo simulation (CSMCS) method is implemented for comparison. The convergence criterion of the CSMCS is set to be 4000 simulations [33]. Detailed results are provided, as shown in Table V.

As Table V shows, the annual reliability indices yielded by these two methods are relatively close. The average relative errors of the annual PLC, EFLC, and EENS indices between these two methods are only 1.470%, 0.885%, and 1.589%, respectively, which can be attributed to the stochastic characteristics of the simulations. This observation proves that the two-step acceleration method will not harm the accu-

racy of the system reliability evaluation results.

TABLE V
ANNUAL RELIABILITY INDICES FOR DIFFERENT SCENARIOS

Scenario No.	Method	PLC	EFLC (occurrence/year)	EENS (MWh/year)	CPU time (min)
9	CSMCS	7.253×10^{-4}	1.265	714.424	4451.447
	Proposed	7.369×10^{-4}	1.271	726.380	1089.335
10	CSMCS	2.088×10^{-3}	3.243	2452.769	4642.571
	Proposed	2.116×10^{-3}	3.285	2489.686	1153.805

In terms of computation time, the proposed HT- and MFLL-based method exhibits a remarkable advantage. Compared with CSMCS, the average computational cost can be reduced by 75.334%. The proposed HT- and MFLL-based method is also applied to MRTS-96 to further validate its efficiency and scalability for large systems [39] (detailed results are provided in Supplementary Material B). The results demonstrate that the proposed HT- and MFLL-based method can achieve satisfactory accuracy, which is nearly equivalent to that of CSMCS while maintaining acceptable computation time. This high computational efficiency allows for the proposed HT- and MFLL-based method to capture the effects of random components and aging failures, making it well-suited for practical applications.

D. Accuracy Analysis of Simulated Component State Sequences

This case study verifies the accuracy of the simulated component state sequences. To achieve this, the failure inversion method proposed in [40] is employed, whose fundamental concept is to compare the aging-related failure rates of components derived from the simulation results with the statistical values (treated as true values). The inversion times for each component type are set to be 500. Detailed comparison results of the three component types are given in Table VI.

TABLE VI
COMPARISON RESULTS OF THREE COMPONENT TYPES

Component type	Asset age (year)	Aging-related failure rate (time/year)	
		Calculated value	True value
Generating unit	48	0.020	0.019
	51	0.072	0.072
	54	0.180	0.171
Power transformer	42	0.185	0.190
	47	0.271	0.277
	55	0.358	0.364
Transformer line	45	0.041	0.040
	50	0.084	0.083
	55	0.149	0.146

It can be observed from Table VI that there is a negligible discrepancy between the aging-related failure rates (calculated value) and the statistical results (true value) for all three component types. The average relative errors across the three asset ages are only 3.502%, 2.338%, and 1.735%, respectively, which validates the accuracy of the proposed three-state component reliability model in simulating the state transition process and failure behavior of aged components.

E. Application in System Reliability Analysis with Renewable Energy Resource Integration

Renewable energy resources are becoming increasingly prevalent in modern power systems. Nevertheless, component aging, such as transmission network aging, may significantly impede the transmission and full utilization of renewable energy resources, thereby posing a threat to the system reliability [41]. Because the transmission network of the MRTS-79 is too reliable, this subsection uses a modified IEEE Roy Billinton test system with wind power integration (defined as MRBTS) to analyze the impact of component aging failures on system reliability.

The original Roy Billinton test system (RBTS) includes 6 buses and 11 generating units. The total installed capacity is 240 MW, with a system peak load of 185 MW [42]. In the MRBTS, both bus 1 and bus 2 have one 40 MW generating unit replaced by wind turbines. The RTS 8736-hour load data are still used as the annual system load data. The wind speed of a provincial system in China is used to obtain the annual output curve of the wind turbines [42]. In the reliability evaluation process, system states with the same component state vectors may result in different MFLL values due to variations in renewable energy output. To maintain the effectiveness of the two-step acceleration method, an MFLL correction step is introduced to determine the individual MFLL values associated with system states having the same component states but varying renewable energy outputs [43]. Details can be found in Supplementary Material C.

For comparison purposes, the following two scenarios are provided. In scenario 1, the system is assumed to be free from aging failure effects, while in scenario 2, the asset ages of the generating units and transmission lines are set to be 54 and 55 years, respectively. To ensure a fair comparison, it is assumed that the two wind turbines do not experience any failures in the two scenarios. The detailed results are provided in Table VII.

TABLE VII
ANNUAL RELIABILITY INDICES FOR TWO SCENARIOS

Scenario No.	PLC	EFLC (occurrence/year)	EENS (MWh/year)
1	1.338×10^{-3}	0.4362	145.304
2	4.903×10^{-3}	1.6310	539.928

As indicated in Table VII, compared with those in scenario 1, the PLC, EFLC, and EENS indices in scenario 2 increase by 2.664, 2.739, and 2.716 times, respectively. This observation highlights the negative impact of component aging on the reliability of power systems integrated with renewable energy resources.

F. Application in Spare Component Analysis

Given the critical role of generating units in power systems [44], this subsection describes the investigation and quantification of the impact of the number of generating units on system reliability using the proposed SMCS-based system reliability evaluation method. To ensure a fair comparison, the asset ages of the power transformers and transmission lines are fixed at 52 and 55 years, respectively. It is assumed that spare generating units could replace any failed unit within the system. The annualized PLC and EENS indices under different asset ages of aging generating units and varying numbers of spare generating units are provided, as shown in Figs. 8 and 9.

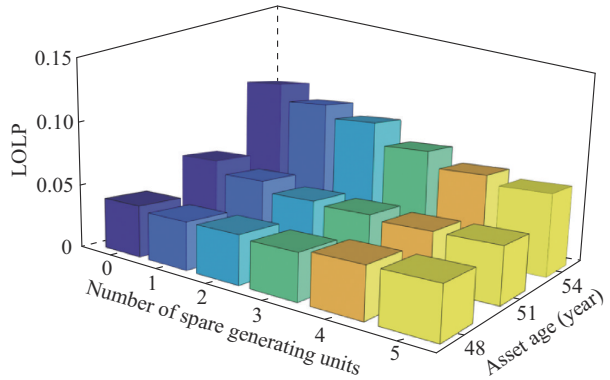

Fig. 8. Annualized PLC indices under different asset ages of aging generating units and varying numbers of spare generating units.

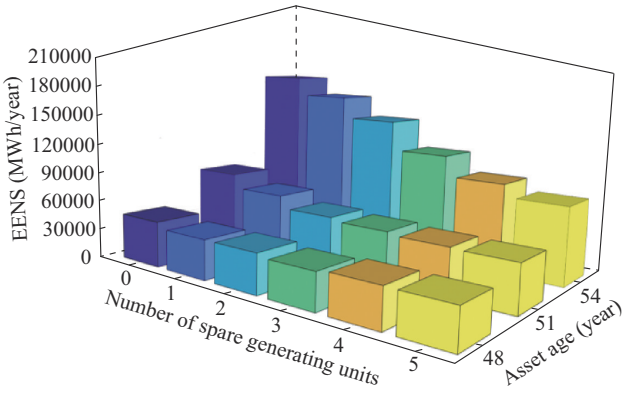

Fig. 9. Annualized EENS indices under different asset ages of aging generating units and varying numbers of spare generating units.

According to Fig. 8 and Fig. 9, it can be concluded that both the PLC and EENS indices greatly decrease as the number of spare generating units increases. For example, when the spare generating units are 54 years old, the implementation of five spare generating units can lead to notable reductions of 59.197% and 50.762% in the PLC and EENS indices, respectively. This is because the application of spare generating units can substantially shorten the time required for replacing the aging-failed generating units, thereby reducing the system outage duration. This observation proves that the implementation of spare component planning is a significant measure for mitigating the negative impact of component aging failures on system reliability. The results also demonstrate the capacity of the proposed SMCS-based system reliability evaluation method as a reliability quantification tool for system reliability optimization.

VI. Discussion

As illustrated in Table I, there are obvious differences in causal factors between random failure and aging failure modes of a component. The specific causal factors of these two failure modes depend on the type and structure of the studied component. For instance, random failures in transmission lines are caused mainly by external factors such as tree contact, bird contact, lightning, and rainstorms, while aging failures typically result from the corrosion of metal parts, insulation damage, and partial discharge. For transformers, random failures often include lightning strikes, tap changer failures, and external short circuits, whereas aging failures are primarily due to the irreversible degradation of insulating paper. Detailed discussions on this topic can be found in [45], [46]. Moreover, it is worth emphasizing that this paper focuses on the whole asset when modeling component non-repairable aging failures. Specifically, it follows the assumption that the assets experiencing aging failures need to be completely replaced with new assets. However, aging failures may render certain subcomponents of an asset unrepairable, necessitating their replacement while allowing for the remaining subcomponents to be used. In response, a potential future solution is to independently build a three-state component reliability model of subcomponents. Additionally, the failure basis for the proposed three-state component reliability model needs to be further enhanced in the future to support more robust model justification.

Furthermore, in practical situations, many power assets are scrapped due to preventive management across utilities, which increases the difficulty in collecting enough failure statistics data to construct an accurate lifetime distribution for a given component type. This may limit the practical application of the proposed three-state component reliability model in engineering. To overcome this issue, two feasible solutions, namely, aging failure data restoration and all-information methods, have been proposed in previous studies [47], [48]. The first method focuses on converting the collected scrapping age data of power components into their aging-related lifetime through remaining useful lifetime forecasting. The second method is used to construct a lifetime distribution based on all the information in a component group, including both failed and surviving components. Since the proposed three-state component reliability model is completely decoupled from these distribution acquisition methods, both methods can be used in practice.

VII. Conclusion

In this paper, an SMCS-based system reliability evaluation method for incorporating multiple component failure modes in a system reliability evaluation is presented. Compared with previous works, we can conclude:

1) The proposed method can efficiently quantify the comprehensive impact of random failures and non-repairable aging failures on component system reliability, providing more

credible estimations of system reliability indices compared with conventional methods.

2) The proposed three-state component reliability model can describe and distinguish the impacts of the random and aging failure behaviors of a component, making the component state sequence generations more consistent with their actual operation process.

3) The developed two-step acceleration method can enhance the computational performance of the proposed method, making the proposed method more practical and promising for real-world applications, particularly for the systems with a large number of aged components and renewable energy.

4) The proposed method can serve as a valuable reliability quantification tool for planners to support decision-making and the implementation of reliability-centered system maintenance strategies, e.g., spare component optimization.

Future studies can concentrate on developing effective reliability-centered asset management strategies that are based on the established method to enhance the reliability of aged power systems.

REFERENCES

[1] V. Smil, *Creating the Twentieth Century*: *Technical Innovations of 1867-1914 and Their Lasting Impact*. New York: Oxford University Press, 2005, pp 32-97.

[2] M. Kanabar, J. McDonald, and P. Parikh, "Grid innovations and digital transformation: grid innovations and digital transformation of power substations are accelerating the energy transition for global utilities," *IEEE Power and Energy Magazine*, vol. 20, no. 2, pp. 83-95, Mar, 2022.

[3] W. Li, *Reliability Assessment of Electric Power Systems Using Monte Carlo Methods*. New York: Springer Science & Business Media, 2013, pp. 255-296.

[4] R. S. Charrusmitha, N. A. Kumar, and K. Anisha, "An enumerative analysis of major power blackouts in Asian region in the last two decades," *World Journal of Advanced Engineering Technology and Sciences*, vol. l1, no. 2, pp. 522-528, Apr. 2024.

[5] A. D. Stringer, C. C. Thompson, and C. I. Barriga, "Analysis of historical transformer failure and maintenance data: effects of era, age, and maintenance on component failure rates," *IEEE Transactions on Industry Applications*, vol. 55, no. 6, pp. 5643-5651, Aug. 2019.

[6] W. Li, *Risk Assessment of Power Systems: Models, Methods, and Applications*. Hoboken: John Wiley & Sons, 2014, pp. 61-70.

[7] S. K. E. Awadalla, J. V. Milanovic, Z. Wang *et al*., "Overview of power system reliability assessment considering age related failure of equipment," in *Proceedings of 2015 IEEE PES General Meeting*, Denver, USA, Jul. 2015, pp. 1-6.

[8] W. Li, "Incorporating aging failures in power system reliability evaluation," *IEEE Transactions on Power Systems*, vol. 17, no. 3, pp. 918-923, Aug. 2002.

[9] M. S. Alvarez-Alvarado and D. Jayaweera, "Bathtub curve as a Markovian process to describe the reliability of repairable components," *IET Generation, Transmission & Distribution*, vol. 12, no. 21, pp. 5683-5689, Nov. 2018.

[10] M. S. Alvarez-Alvarado and D. Jayaweera, "Operational risk assessment with smart maintenance of power generators," *International Journal of Electrical Power & Energy Systems*, vol. 117, p. 105671, May 2020.

[11] S. Peyghami and F. Blaabjerg, "Availability modeling in power converters considering components aging," *IEEE Transactions on Energy Conversion*, vol. 35, no. 4, pp. 1981-1984, Aug. 2020.

[12] H. Lei and C. Singh, "Non-sequential monte carlo simulation for cyber-induced dependent failures in composite power system reliability evaluation," *IEEE Transactions on Power Systems*, vol. 32, no. 2, pp. 1064-1072, May 2017.

[13] S. Peyghami, M. Fotuhi-Firuzabad, and F. Blaabjerg, "Reliability evaluation in microgrids with non-exponential failure rates of power units," *IEEE Systems Journal*, vol. 14, no. 2, pp. 2861-2872, Nov. 2020.

[14] W. A. Vasquez and D. Jayaweera, "Methodology for overhead conductor replacement considering operational stress and aging characteristics," in *Proceedings of 2018 IEEE PES General Meeting (PESGM)*, Portland, USA, Aug. 2018, pp. 1-5.

[15] H. Kim and C. Singh, "Reliability modeling and simulation in power systems with aging characteristics," *IEEE Transactions on Power Systems*, vol. 25, no. 1, pp. 21-28, Sept. 2010.

[16] K. Xie and W. Li, "Analytical model for unavailability due to aging failures in power systems," *International Journal of Electrical Power & Energy Systems*, vol. 31, no. 7-8, pp. 345-350, Sept. 2009.

[17] Y. Zhao, Y. Tang, W. Li *et al*., "Composite power system reliability evaluation based on enhanced sequential cross-entropy Monte Carlo simulation," *IEEE Transactions on Power Systems*, vol. 34, no. 5, pp. 3891-3901, Apr. 2019.

[18] E. Tómasson and L. Söder, "Improved importance sampling for reliability evaluation of composite power systems," *IEEE Transactions on Power Systems*, vol. 32, no. 3, pp. 2426-2434, Oct. 2017.

[19] M. Kamruzzaman, N. Bhusal, and M. Benidris, "A convolutional neural network-based approach to composite power system reliability evaluation," *International Journal of Electrical Power & Energy Systems*, vol. 135, p. 107468, Feb. 2022.

[20] M. Buhari, V. Levi, and S. K. E. Awadallah, "Modelling of ageing distribution cable for replacement planning," *IEEE Transactions on Power Systems*, vol. 31, no. 5, pp. 3996-4004, Nov. 2016.

[21] A. M. L. da Silva and L. F. Araújo, "Reliability evaluation of generating systems considering aging processes," *Electric Power Systems Research*, vol. 202, p. 107589, Jan. 2022.

[22] H. A. R. Ardabili, M. R. Haghifam, and S. M. Abedi, "A stochastic Markov model for maintenance scheduling in the presence of online monitoring system," *IEEE Transactions on Power Delivery*, vol. 37, no. 4, pp. 2831-2842, Oct. 2022.

[23] C. L. Anderson and M. Davison, "An aggregate Weibull approach for modeling short-term system generating capacity," *IEEE Transactions on Power Systems*, vol. 20, no. 4, pp. 1783-1789, Oct. 2005.

[24] A. M. L. d. Silva, J. G. d. C. Costa, K. G. Machado *et al*., "Probabilistic method for optimizing the number and timing of substation spare transformers," *IEEE Transactions on Power Systems*, vol. 30, no. 4, pp. 2004-2012, Sept. 2015.

[25] J. Mi, Y. Li, Y. Yang *et al*., "Reliability assessment of complex electromechanical systems under epistemic uncertainty," *Reliability Engineering & System Safety*, vol. 152, pp. 1-15, Aug. 2016.

[26] W. Huang, C. Shao, M. Dong *et al*., "Modeling the aging-dependent reliability of transformers considering the individualized aging threshold and lifetime," *IEEE Transactions on Power Delivery*, vol. 37, no. 6, pp. 4631-4645, Feb. 2022.

[27] M. Dong and A. B. Nassif, "Combining modified weibull distribution models for power system reliability forecast," *IEEE Transactions on Power Systems*, vol. 34, no. 2, pp. 1610-1619, Oct. 2019.

[28] S. Li, T. Ding, C. Mu *et al*., "A machine learning-based reliability evaluation model for integrated power-gas systems," *IEEE Transactions on Power Systems*, vol. 37, no. 4, pp. 2527-2537, Nov. 2022.

[29] R. E. Brown, *Electric Power Distribution Reliability*. Boca Raton: CRC Press, 2017, pp. 162-184.

[30] A. C. G. Melo, M. V. F. Pereira, and A. M. L. D. Silva, "A conditional probability approach to the calculation of frequency and duration indices in composite reliability evaluation," *IEEE Transactions on Power Systems*, vol. 8, no. 3, pp. 1118-1125, Aug. 1993.

[31] K. Hou, H. Jia, X. Xu *et al*., "A continuous time markov chain based sequential analytical approach for composite power system reliability assessment," *IEEE Transactions on Power Systems*, vol. 31, no. 1, pp. 738-748, Jan. 2016.

[32] R. N. Allan, *Reliability Evaluation of Power Systems*. Berlin, Germany: Springer Science & Business Media, 2013, pp. 172-209.

[33] Z. Shu, P. Jirutitijaroen, A. M. L. D. Silva *et al*., "Accelerated state evaluation and Latin Hypercube sequential sampling for composite system reliability assessment," *IEEE Transactions on Power Systems*, vol. 29, no. 4, pp. 1692-1700, Jan. 2014.

[34] S. Wang, Z. Li, L. Wu *et al*., "New metrics for assessing the reliability and economics of microgrids in distribution system," *IEEE Transactions on Power Systems*, vol. 28, no. 3, pp. 2852-2861, Mar. 2013.

[35] G. H. Reddy, A. N. Koundinya, M. Raju *et al*., "Lifetime estimation of electrical equipment in distribution system using modified 3-parameter Weibull distribution," in *Proceedings of 2021 International Conference on Design Innovations for 3Cs Compute Communicate Control (ICDI3C)*, Bangalore, India, Jun. 2021, pp. 21-26.

[36] D. Zhou, Z. Wang, P. Jarman *et al*., "Data requisites for transformer

statistical lifetime modelling – part II: combination of random and aging-related failures," *IEEE Transactions on Power Delivery*, vol. 29, no. 1, pp. 154-160, Jul. 2014.
[37] G. A. Hamoud, "Assessment of spare transformer requirements for high voltage load stations," in *Proceedings of 2012 IEEE PES General Meeting*, San Diego, USA, Jul. 2012, pp. 1-8.
[38] R. J. Schweiner, K. E. Twomey, and K. E. Lindsey, "Transmission line emergency restoration philosophy at Los Angeles department of water and power," in *Proceedings of 2003 IEEE 10th International Conference on Transmission and Distribution Construction, Operation and Live-Line Maintenance*, Orlando, USA, Apr. 2003, pp. 11-17.
[39] C. Grigg, P. Wong, P. Albrecht *et al.*, "The IEEE reliability test system-1996. A report prepared by the reliability test system task force of the application of probability methods subcommittee," *IEEE Transactions on Power Systems*, vol. 14, no. 3, pp. 1010-1020, Aug. 1999.
[40] J. Zhong, "Asset management strategies of circuit breakers considering ageing failures and system risk," Ph.D. dissertation, Department of Electrical Engineering, Chongqing University, Chongqing, China, 2017.
[41] G. Sansavini, R. Piccinelli, L. R. Golea *et al*., "A stochastic framework for uncertainty analysis in electric power transmission systems with wind generation," *Renewable Energy*, vol. 64, pp. 71-81, Apr. 2014.
[42] X. Li, K. Xie, C. Shao *et al*., "A region-based approach for the operational reliability evaluation of power systems with renewable energy integration," *IEEE Transactions on Power Systems*, vol. 39, no. 2, pp. 3389-3340, Jun. 2023.
[43] X. Li K. Xie, C. Shao *et al.*, "A sensitivity-based rolling operational reliability evaluation that follows the changing available generation capacity of renewable energies," *IEEE Transactions on Power Systems*, doi: 10.1109/TPWRS.2024.3379646
[44] N. W. Hodges, "Improving generator availability by use of strategic spares," *Power Engineering Journal*, vol. 3, no. 5, pp. 257-262, Sept. 1989.
[45] C. Aj, M. A. Salam, Q. M. Rahman *et al*., "Causes of transformer failures and diagnostic methods – a review," *Renewable and Sustainable Energy Reviews*, vol. 82, pp. 1442-1456, Feb. 2018.
[46] C. M. Chu, J. F. Moon, H. T. Lee *et al*., "Extraction of time-varying failure rates on power distribution system equipment considering failure modes and regional effects," *International Journal of Electrical Power & Energy Systems*, vol. 32, no. 6, pp. 721-727, Jul. 2010.
[47] W. Huang, C. Shao, B. Hu *et al.*, "A restoration-clustering-decomposition learning framework for aging-related failure rate estimation of distribution transformers," *Reliability Engineering & System Safety*, vol. 232, p. 109043, Apr. 2023.
[48] W. Li, "Evaluating mean life of power system equipment with limited end-of-life failure data," *IEEE Transactions on Power Systems*, vol. 19, no. 1, pp. 236-242, Feb. 2004.

Wei Huang received the B.S. degree from China University of Petroleum, Qingdao, China, in 2019. He is currently pursuing the Ph.D. degree in the School of Electrical Engineering of Chongqing University, Chongqing, China. His research interests include power system planning, operation, and asset management.

Bo Hu received the Ph.D. degree in electrical engineering from Chongqing University, Chongqing, China, in 2010. He is now a Professor with the School of Electrical Engineering, Chongqing University. His main research interests include power system reliability, planning, and analysis.

Changzheng Shao received the B.S. degree in electrical engineering from Shandong University, Jinan, China, and the Ph.D. degree in electrical engineering from Zhejiang University, Hangzhou, China, in 2015 and 2020, respectively. He is currently an Assistant Professor at Chongqing University, Chongqing, China. His research interests include operation optimization and reliability evaluation of integrated energy system.

Wei Li received the B.S. and M.S. degrees in electrical engineering from Tsinghua University, Beijing, China, in 2016 and 2018, respectively. He is currently an Engineer of power distribution with the Electric Power Research Institute, China Southern Power Grid, Guangzhou, China. His research interests include smart distribution system, distribution network dispatch, and integration of distributed generation into electric power systems.

Xiaozhe Wang received the B.S. degree in information science and electronic engineering from Zhejiang University, Zhejiang, China, in 2010, and the Ph.D. degree from the School of Electrical and Computer Engineering, Cornell University, Ithaca, USA, in 2015. She is currently an Associate Professor with the Department of Electrical and Computer Engineering, McGill University, Montreal, Canada. Her research interests include power system stability and control, uncertainty quantification in power system security and stability, and wide-area measurement system-based detection, estimation, and control.

Kaigui Xie received the Ph.D. degree in power system and its automation at Chongqing University, Chongqing, China, in 2001. Currently, he is a Full Professor in the School of Electrical Engineering, Chongqing University. His main research interests include power system reliability, planning, and analysis.

C. Y. Chung is currently the Head of Department and Chair Professor of Power Systems Engineering in the Department of Electrical Engineering at the Hong Kong Polytechnic University, Hong Kong, China. His research interests include smart grid technology, renewable energy, power system stability/control, planning and operation, computational intelligence application, electricity market, and electric vehicle charging.